Supporting Information for 10.1021/acs.jpclett.8b00023

Photochemistry of the Simplest Criegee Intermediate, CH_2OO: Photoisomerization Channel toward Dioxirane Revealed by CASPT2 calculations and Trajectory Surface-Hopping Dynamics

Yazhen Li[1], Qianqian Gong[1], Ling Yue[2], Wenliang Wang[1,*] and Fengyi Liu[1,*]

1. Key Laboratory for Macromolecular Science of Shaanxi Province, School of Chemistry & Chemical Engineering, Shaanxi Normal University, Xi'an, Shaanxi 710062, P. R. China
2. School of Sciences, Xi'an Jiaotong University, Xi'an, Shaanxi 710049, P. R. China

INDEX

Computational Details

Cartesian Coordinate of Important Geometries

Computational Details

Electronic-Structure Calculations

We carried out the SA8-CASSCF(14*e*,10*o*)/ANO-RCC-VTZP geometry optimizations without symmetric constraints, which allows for the simultaneous description of X^1A, A^1A and B^1A states (respectively corresponding to the X^1A′, A^1A″ and B^1A′ states under C_s symmetry). The eight-state averaged wavefunction is used to sufficiently describe both the H_2CO X^1A_1 + O ^{1}D and H_2CO a^3A″ + O ^{3}P channels. The active orbitals in CAS(14*e*,10*o*), as shown in Figure S1, including three π orbitals, σ/σ* orbitals of C-O and O-O bonds, 2s orbitals of oxygen atoms, and a lone-pair orbital of terminal oxygen. We respectively calculated the X^1A, A^1A and B^1A states PECs by relaxed scanning along the O-O distance. Note: For A^1A-PEC, the geometries at 1.4~1.8 Å are obtained by applying an additional planar-constraint, otherwise they will decay along the C-O torsional mode to perpendicular structures. The C_1-PECs computed in this study (shown in Figure 2) qualitatively reproduce the DW-CASSCF(12*e*,11*o*)-computed C_s-PECs [1]. Thus, it provides a solid base for further explorations of 2-D PESs.

To describe the possible out-of-plane motion, we further carried out 2-D scanning of PESs for X^1A, A^1A and B^1A states, choosing the H-C-O1-O2 dihedral angle (ϕ) and C-O2 distance as independent variables. The 2-D PESs are calculated at both the CASSCF level (Figure S3 and S4) and MS-CASPT2 level (Figure S5 and S6). The two series of PESs show essentially the same topology except for some qualitative differences. On ground-state surface, the Criegee intermediate (*X*-CH_2OO) and dioxirane (*X*-Dioxirane) is interlinked by a transition state (*X*-TS); the barrier from *X*-CH_2OO side, 20.7 kcal/mol (at MS-CASPT2 level), is in good consistent with previously reported value (19.66 kcal/mol) at the CCSD(T)/aug-cc-pVTZ level [2] and 19.0 kcal/mol at the CCSD(T)-F12a/AVTZ level [3].

The CASSCF and CASPT2 calculations were done by MOLCAS 7.8 package [4,5].

Trajectory Surface-Hopping Dynamics

Trajectory surface hopping nonadiabatic dynamics involved the lowest five singlet states (i.e., X^1A, A^1A and B^1A, etc.) are carried out using SHARC [6-8] (Surface Hopping in the Adiabatic

Representation Including Arbitrary Couplings) program suite interfaced with MOLPRO [9] quantum chemistry package. In the surface hopping approach, the nuclei move in a particular electronic state according to the Newton's equations, while electronic wavefunction is propagated using the time-dependent electronic Schrödinger equation that considers the nonadiabatic couplings between different electronic states. At near quasi-degenerate regions, the trajectory may switch from one state to another based on the electronic wavefunction and a stochastic algorithm.

The distribution of initial atomic coordinates and velocities are obtained using a quantum-harmonic Wigner sampling [10]. A total of 120 trajectories are initially populated to the A^1A state, using an energy window of 0-3 eV for exciting. Starting from the A^1A state, the trajectories are running with energies and gradients being computed on-the-fly by MOLPRO. The nuclear coordinates are updated according to the Velocity Verlet algorithm [11] with a timestep of 0.2 fs. The MCH representations of electronic states implemented in SHARC, which is the basis of the eigenfunctions of the molecular Coulomb Hamiltonian, are used. Technical details of the simulations can be refers to ref. 4-6. Finally, 74 trajectories are successfully finished, which are evaluated in the photodynamics of Criegee intermediate.

The energies and gradients for nonadiabatic dynamics simulations are calculated at the CASSCF level, with the CAS(14*e*,10*o*) active space (same to that for electronic-structure calculations) and a smaller def-SVP basis set, using the MOLPRO program.

References:

(1) Dawes, R.; Jiang, B.; Guo, H. *J. Am. Chem. Soc.* **2015**, *137*, 50.

(2) Kalinowski, J.; Räsänen, M.; Heinonen, P.; Kilpeläinen, I.; Gerber, R. B. *Angew. Chem. Int. Ed.* **2014**, *53*, 265.

(3) Li, J.; Carter, S.; Bowman, J. M.; Dawes, R.; Xie, D.; Guo, H. *J. Phys. Chem. Lett*. **2014**, *5*, 2364.

(4) Karlström, G.; Lindh, R.; Malmqvist, P.-Å.; Roos, B. O.; Ryde, U.; Veryazov, V.; Widmark, P.-O.; Cossi, M.; Schimmelpfennig, B.; Neogrady, P.; et al. MOLCAS: A Program Package for Computational Chemistry. *Comput. Mater. Sci.* **2003**, *28*, 222–239.

(5) Aquilante, F.; De Vico, L.; Ferré, N.; Ghigo, G.; Malmqvist, P.-Å.; Neogrády, P.; Pedersen, T. B.; Pitoňák, M.; Reiher, M.; Roos, B. O.; et al. MOLCAS 7: The Next Generation. *J. Comput. Chem.* **2010**, *31*, 224–247.

(6) Mai, S.; Richter, M.; Ruckenbauer, M.; Oppel, M.; Marquetand, P.; González, L. *sharc-md.org*. **2014**.

(7) Richter, M.; Marquetand, P.; González-Vázquez, J.; Sola, I.; González. L. *J. Chem. Theory. Comput*. **2011**, *7*, 1253.

(8) Mai, S.; Marquetand, P.; González, L. *Int. J. Quantum. Chem.* **2015**, *115*, 1215.

(9) MOLPRO, version 2012.1, a package of ab initio programs, Werner, H.-J.; Knowles, P. J.; Knizia, G.; Manby, F. R.; Schütz, M.; Celani, P.; Korona, T.; Lindh, R.; Mitrushenkov, A.; Rauhut, G.; Shamasundar, K. R.; Adler, T. B.; Amos, R. D.; Bernhardsson, A.; Berning, A.; Cooper, D. L.; Deegan, M. J. O.; Dobbyn, A. J.; Eckert, F.; Goll, E.; Hampel, C.; Hesselmann, A.; Hetzer, G.; Hrenar, T.; Jansen, G.; Köppl, C.; Liu, Y.; Lloyd, A. W.; Mata, R. A.; May, A. J.; McNicholas, S. J.; Meyer, W.; Mura, M. E.; Nicklaß, A.; O'Neill, D. P.; Palmieri, P.; Peng, D.; Pflüger, K.; Pitzer, R.; Reiher, M.; Shiozaki, T.; Stoll, H.; Stone, A. J.; Tarroni, R.; Thorsteinsson, T.; and Wang, M. see http://www.molpro.net.

(10) Wigner, E. *Phys. Rev*. **1932**, *40*, 749.

(11) Verlet L. *Phys. Rev.*, **1967**, *159*, 98–103.

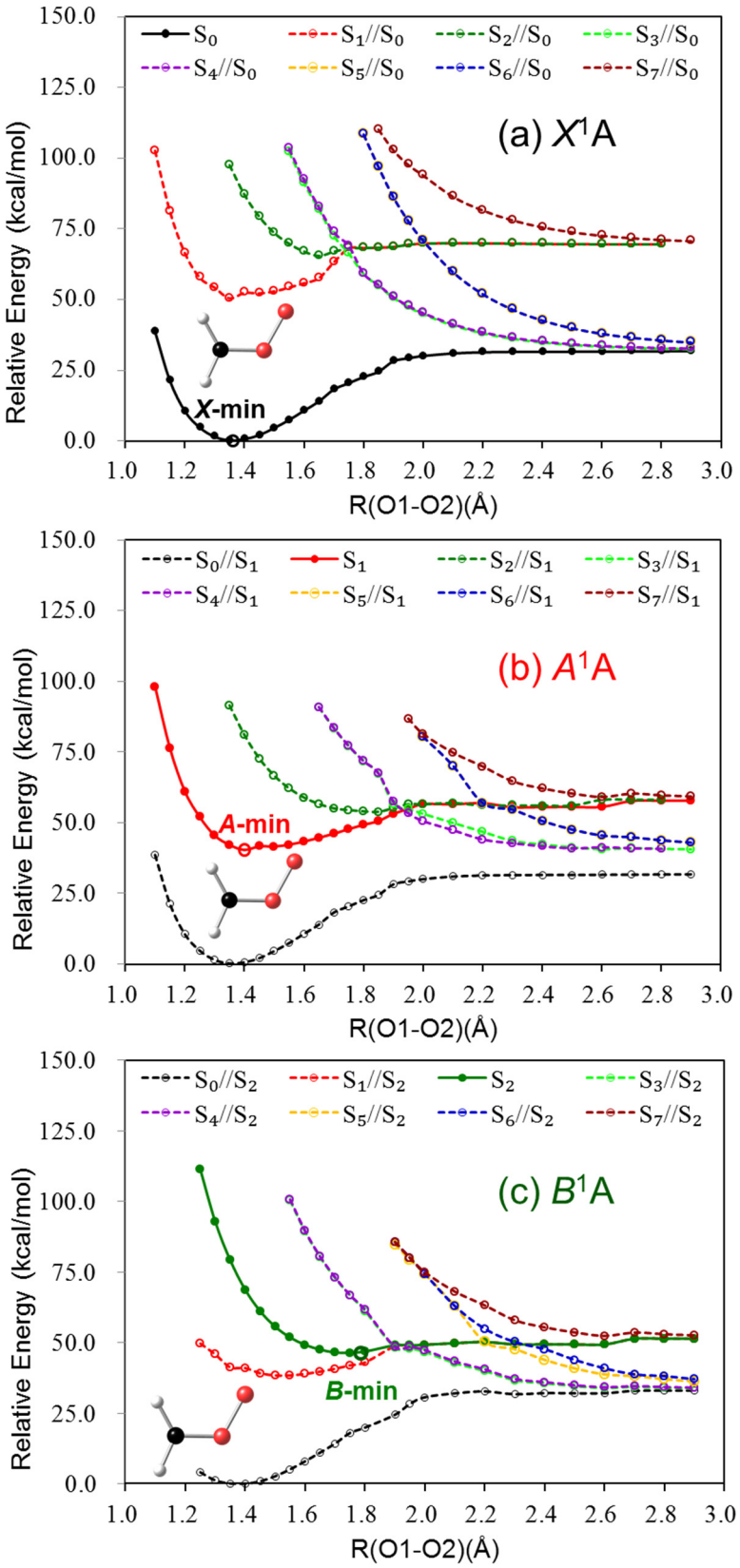

Figure S1. The SA8-CASSCF(14*e*,10*o*)/ANO-RCC-VTZP computed O-O dissociation energy profiles for ground state S_0 (X^1A) and the lowest seven excited singlet states, S_1-S_7. Geometries are optimized on **(a) X^1A**, **(b) A^1A** and **(c) B^1A-state**, respectively. All energies are relative to the ground-state energy of CH_2OO.

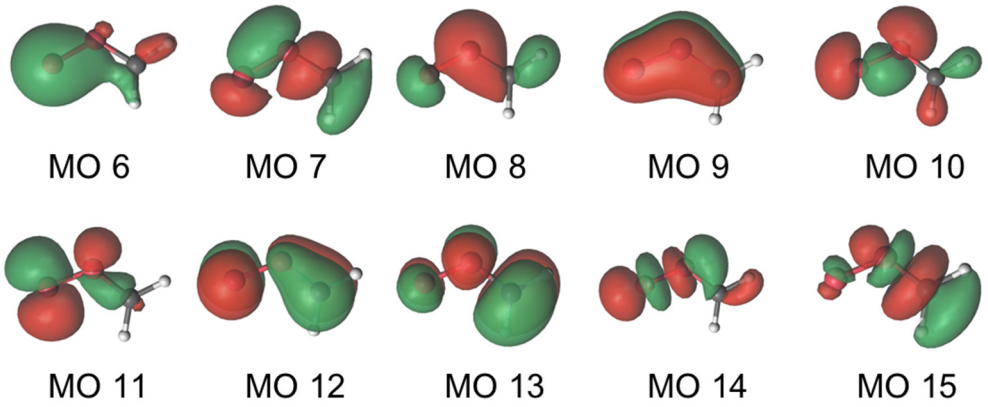

Figure S2. The active orbitals used in the CASSCF(14*e*,10*o*)/ANO-RCC-VTZP calculations.

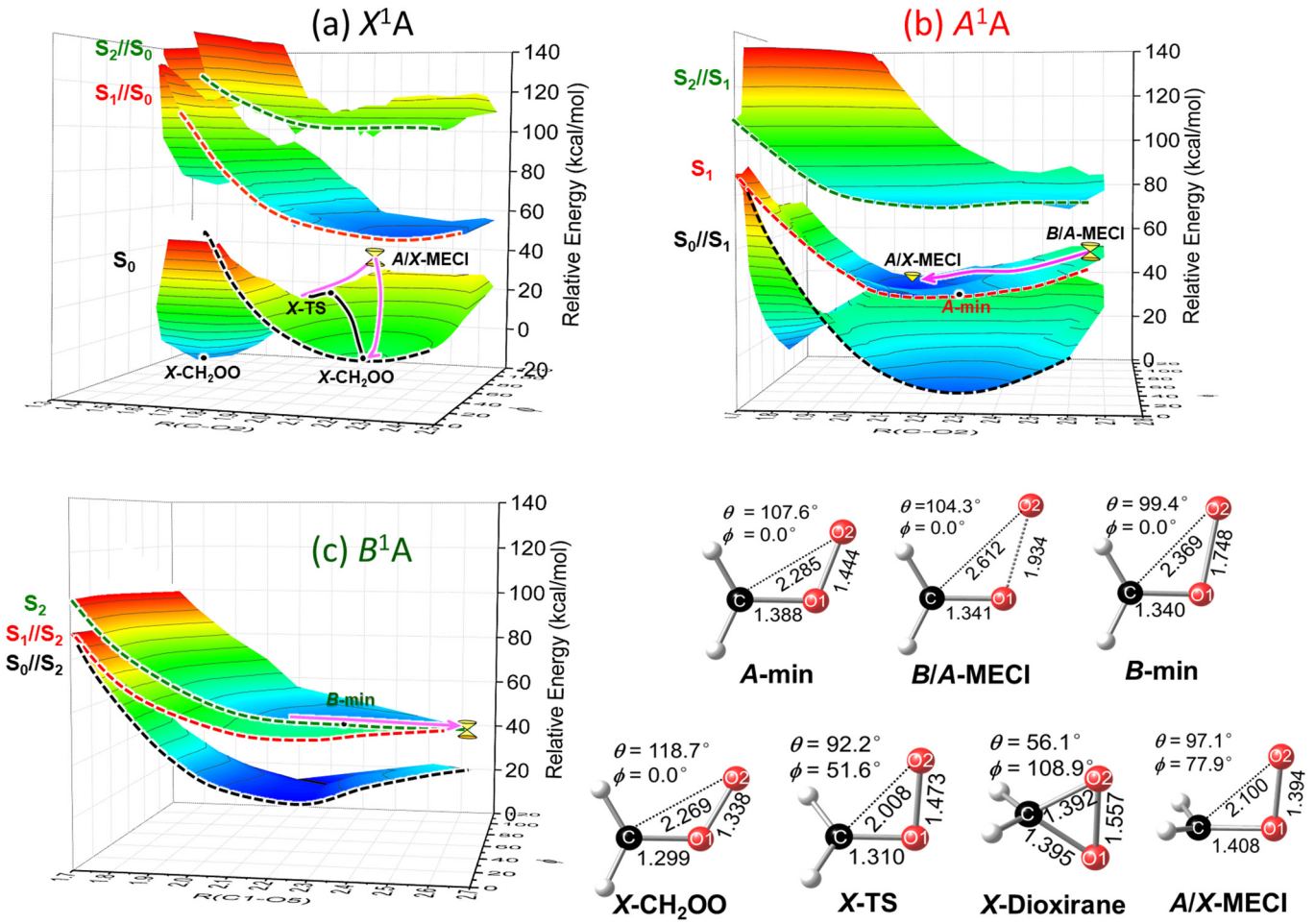

Figure S3. The **CASSCF**(14*e*,10*o*)/ANO-RCC-VTZP computed **(a)** X^1**A**, **(b)** A^1**A** and **(c)** B^1**A-state** PESs with respected to the C-O2 distance and H-C-O1-O2 dihedral angle (ϕ) of CH_2OO. **Optimized geometries of key structures** including minima (min), transition state (TS) and minimal-energy crossing points (MECIs) on the CASSCF-computed PESs are shown.

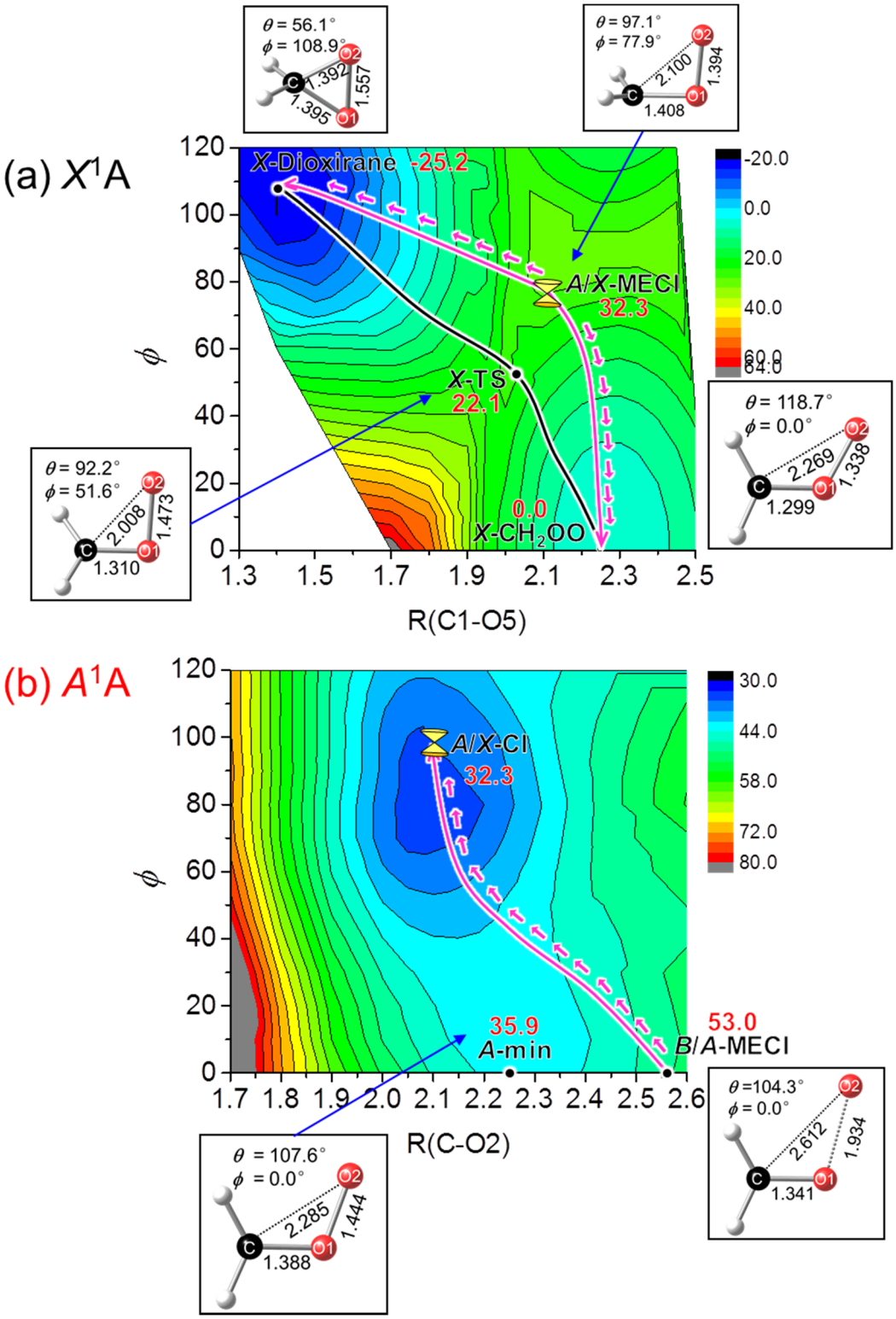

Figure S4. The 2-D contour plots **CASSCF**(14*e*,10*o*)/ANO-RCC-VTZP computed **(a)** X^1**A** and **(b)** A^1**A PESs** with respected to the C-O2 distance and H-C-O1-O2 dihedral angle (ϕ) of CH_2OO. Important geometries are shown with important geometry parameters. The two pink lines respectively shows the of $S_1 \rightarrow S_0$ and $S_2 \rightarrow S_1$ internal conversion paths, while the black line shows the S_0 isomerization path.

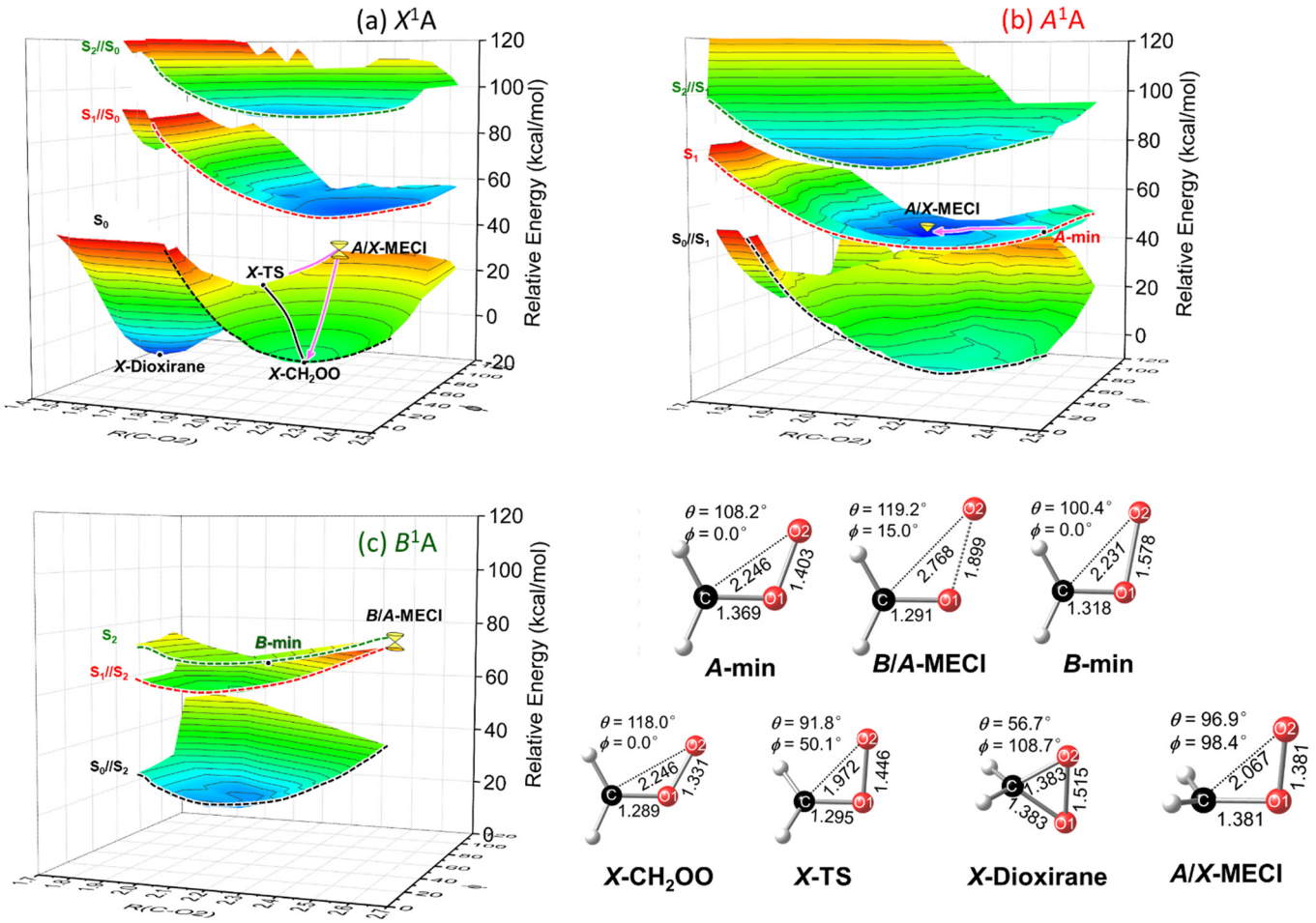

Figure S5. The **MS-CASPT2**(14*e*,10*o*)/ANO-RCC-VTZP computed **(a)** X^1**A**, **(b)** A^1**A** and **(c)** B^1**A-state** PESs with respected to the C-O2 distance and H-C-O1-O2 dihedral angle (ϕ) of CH_2OO. **Optimized geometries of key structures** on the CASPT2-computed PESs are shown.

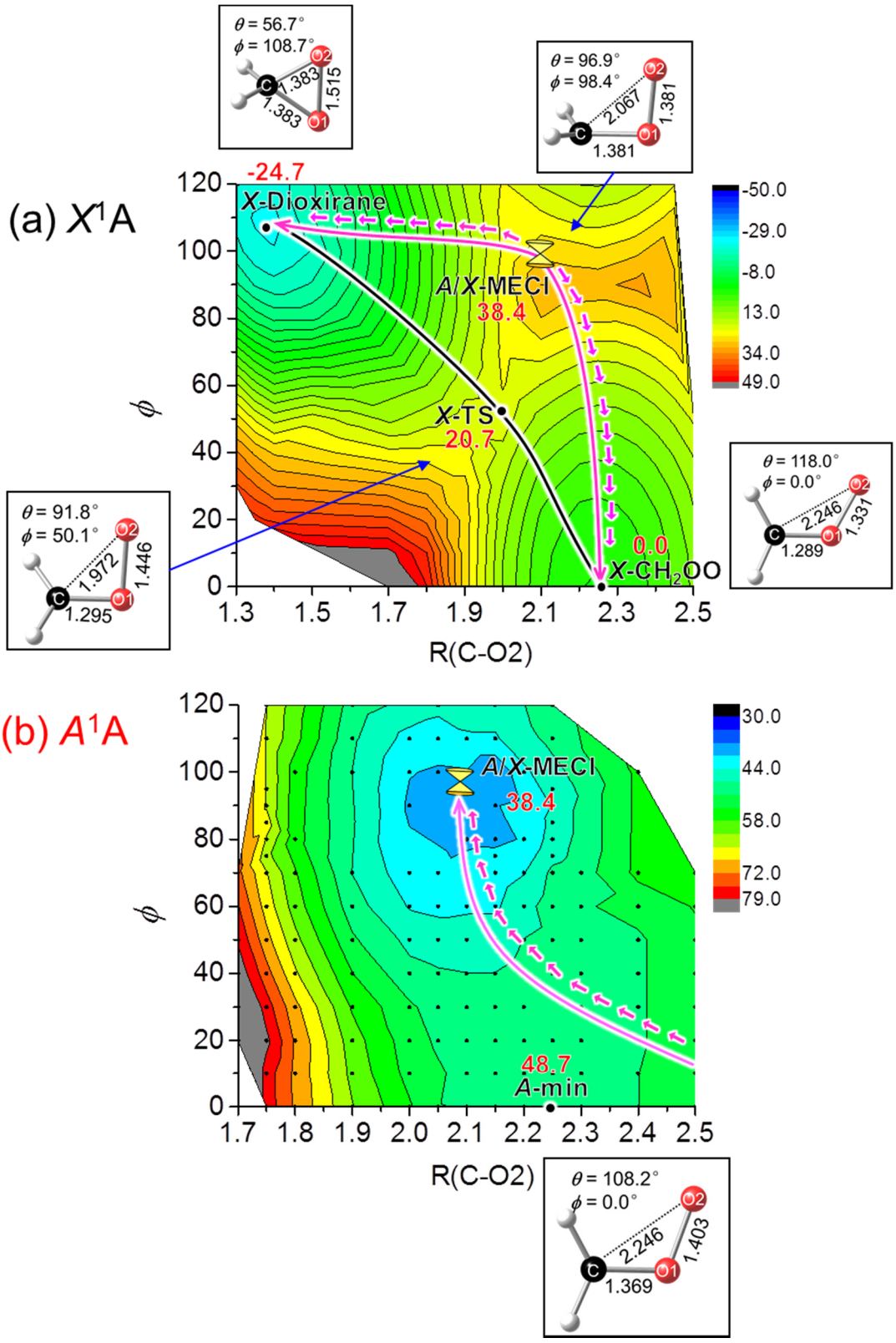

Figure S6. The 2-D contour plots **MS-CASPT2**(14*e*,10*o*)/ANO-RCC-VTZP computed **(a)** X^1**A** and **(b)** A^1**A PESs** with respected to the C-O2 distance and H-C-O1-O2 dihedral angle (ϕ) of CH_2OO. Important geometries are shown with important geometry parameters. The two pink lines respectively shows the of $S_1 \rightarrow S_0$ and $S_2 \rightarrow S_1$ internal conversion paths, while the black line shows the S_0 isomerization path.

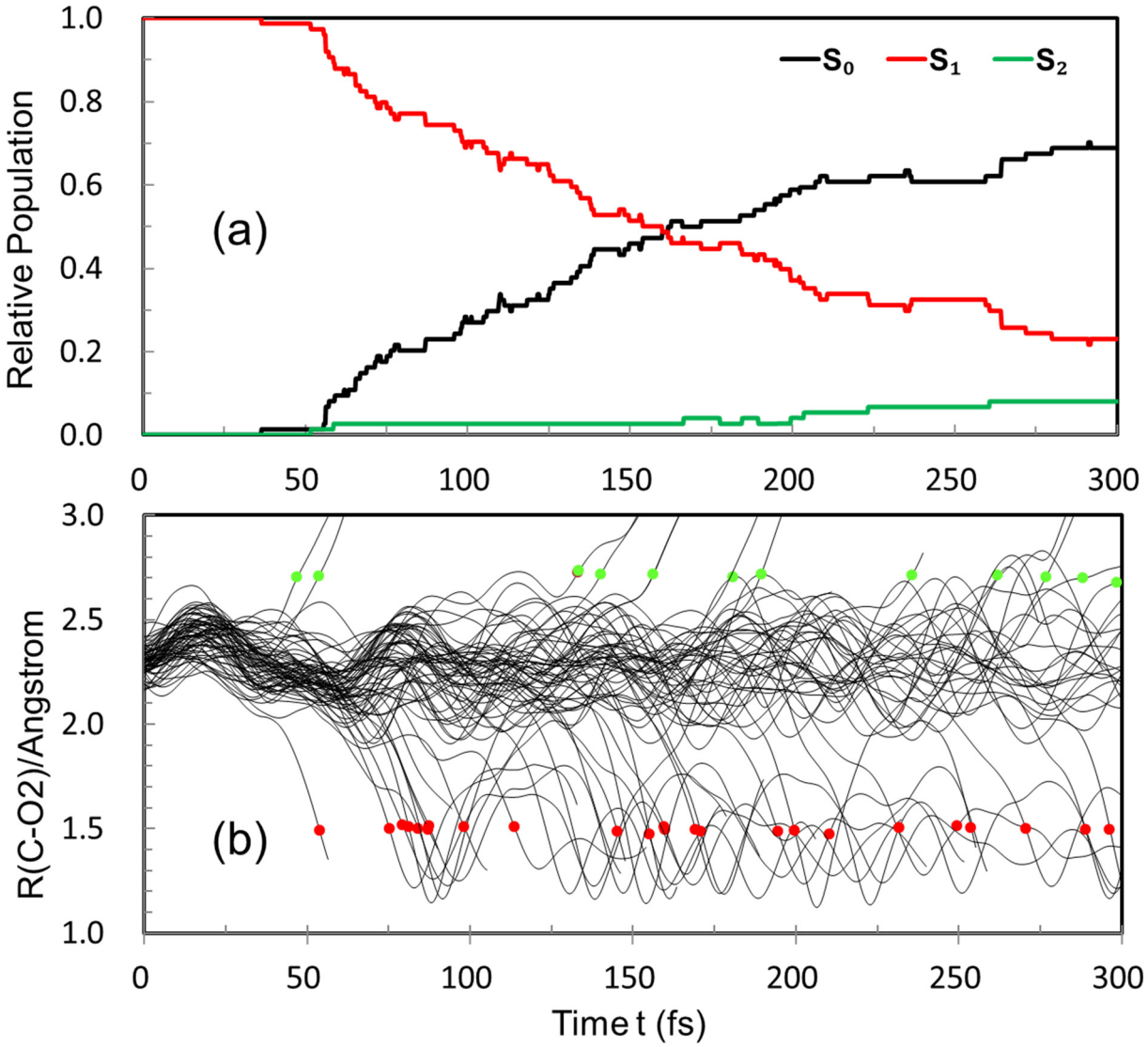

Figure S7. **(a) Quantum populations** for an ensemble of 74 trajectories; **(b) Evolution of C-O2 distance** of the Criegee Intermediate of each trajectory.

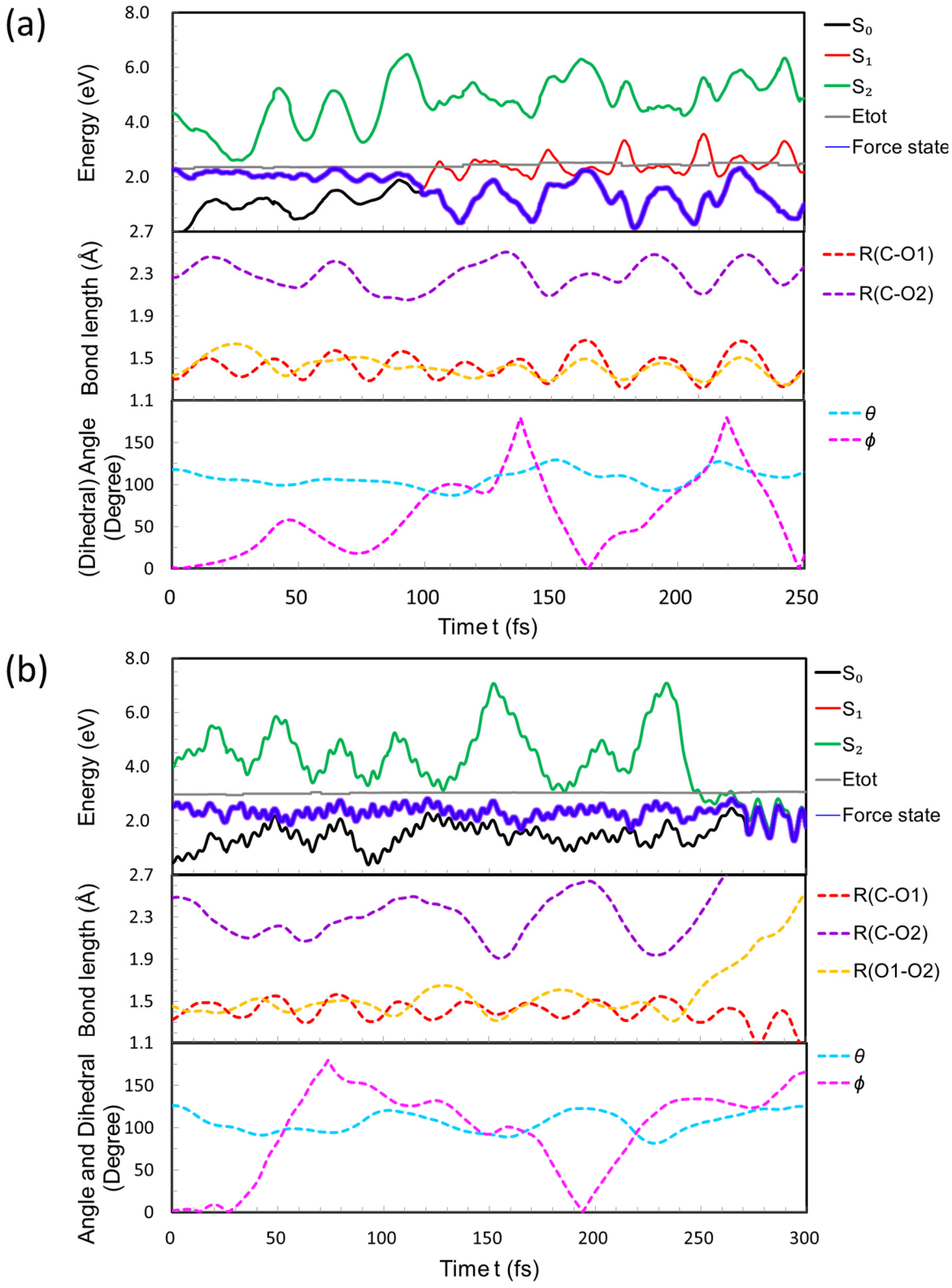

Figure S8. The representive trajectories for **(a) *E-Z* photoisomerization** and **(b) O-O photodissociation**, respectively.

Cartesian Coordinate of Important Geometries

SA8-CASSCF/ANO-RCC-VTZP

***X*-min**

-189.41177719

C	1.0738	-0.2003	-0.0002
H	1.0252	-1.2769	0.0000
H	1.9634	0.4028	0.0002
O	-0.0264	0.4716	0.0000
O	-1.1719	-0.2062	0.0000

***X*-Dioxirane**

-189.43923893

C	0.7893	-0.2464	0.0425
H	1.0804	-1.2380	-0.2646
H	1.5346	0.3403	0.5556
O	-0.0309	0.4437	-0.8307
O	-0.5094	-0.1087	0.4972

***X*-TS**

-189.36693772

C	0.9449	-0.3295	-0.1255
H	1.3223	-1.2547	-0.5262
H	1.4445	0.2178	0.6479
O	-0.1319	0.1621	-0.6497
O	-0.7158	0.3952	0.6535

***A*-min**

-189.33502395

C	1.0853	-0.2050	-0.0004
H	0.9951	-1.2734	0.0000
H	1.9857	0.3760	0.0004
O	-0.0426	0.5717	-0.0002
O	-1.1593	-0.2785	0.0002

***B*-min**

-189.29718054

C	1.0640	-0.1642	-0.0001
H	0.9186	-1.2206	-0.0001
H	2.0119	0.3365	0.0002
O	0.0231	0.6450	-0.0001
O	-1.1536	-0.4057	0.0001

A/X-MECI

-189.33899861

C	1.0009	-0.2828	-0.0125
H	1.2191	-1.2798	-0.3288
H	1.7163	0.3278	0.4881
O	-0.0932	0.3388	-0.5823
O	-0.9796	0.0904	0.4477

B/A-MECI

-189.28085859

C	1.1535	-0.2128	-0.1098
H	1.1383	-1.2712	0.0863
H	2.0729	0.3492	0.0158
O	0.1175	0.5528	-0.0284
O	-1.6114	-0.2302	0.0373

MS3-CASPT2/ANO-RCC-VTZP

***X*-min**

-188.88232398

C	1.0801	-0.2088	0.0000
H	1.0403	-1.2705	0.0000
H	1.9584	0.3866	-0.0001
O	-0.0259	0.4731	0.0003
O	-1.1889	-0.1894	-0.0002

***X*-Dioxirane**

-188.92241404

C	0.7878	-0.2492	0.0501
H	1.0693	-1.2434	-0.2293
H	1.5207	0.3270	0.5761
O	0.0159	0.4474	-0.8761
O	-0.5297	-0.0909	0.4792

***X*-TS**

-188.84705459

C	1.0063	-0.1817	-0.0594
H	0.9616	-1.2353	-0.1714
H	1.8685	0.3273	0.3118
O	-0.0151	0.5491	-0.4322
O	-0.9573	-0.2685	0.3512

***A*-min**

-188.82507482

C	1.0953	-0.2074	-0.0002
H	1.0052	-1.2664	0.0000
H	1.9931	0.3629	0.0001
O	-0.0409	0.5894	0.0000
O	-1.1886	-0.2876	0.0000

***B*-min**

-188.78911086

C	1.0922	-0.1584	0.0000
H	0.9279	-1.2021	0.0001
H	2.0442	0.3158	-0.0001
O	0.0579	0.6930	0.0001
O	-1.2582	-0.4574	-0.0001

***A*/*X*-MECI**

-188.83094953

C	1.0830	-0.2218	-0.1909
H	1.1359	-1.2778	-0.3235
H	1.6479	0.3152	0.5374
O	-0.1345	0.3720	-0.5751
O	-0.8682	0.0033	0.5520

B/A-MECI

-188.79657086

C	1.1413	-0.1498	0.0000
H	0.9809	-1.2044	0.0000
H	2.0968	0.3292	0.0000
O	0.0953	0.6889	0.0000
O	-1.4502	-0.4731	0.0000